The EMBO Journal Vol. 22 No. 23 pp. 6267–6276, 2003

Osteocyte control of bone formation via sclerostin, a novel BMP antagonist

David G.Winkler[1], May Kung Sutherland[1], James C.Geoghegan[1], Changpu Yu[1], Trenton Hayes[1], John E.Skonier[1], Diana Shpektor[1], Mechtild Jonas[2], Brian R.Kovacevich[2], Karen Staehling-Hampton[3], Mark Appleby[4], Mary E.Brunkow[3] and John A.Latham[1,5]

Departments of [1]Gene Function and Target Validation, [2]Molecular Biology, [3]Genomics and [4]Discovery Biology, Celltech R&D, Inc., Bothell, WA 98021, USA

[5]Corresponding author
e-mail: john.latham@celltechgroup.com

D.G.Winkler and M.Kung Sutherland contributed equally to this work

There is an unmet medical need for anabolic treatments to restore lost bone. Human genetic bone disorders provide insight into bone regulatory processes. Sclerosteosis is a disease typified by high bone mass due to the loss of *SOST* expression. Sclerostin, the *SOST* gene protein product, competed with the type I and type II bone morphogenetic protein (BMP) receptors for binding to BMPs, decreased BMP signaling and suppressed mineralization of osteoblastic cells. *SOST* expression was detected in cultured osteoblasts and in mineralizing areas of the skeleton, but not in osteoclasts. Strong expression in osteocytes suggested that sclerostin expressed by these central regulatory cells mediates bone homeostasis. Transgenic mice overexpressing *SOST* exhibited low bone mass and decreased bone strength as the result of a significant reduction in osteoblast activity and subsequently, bone formation. Modulation of this osteocyte-derived negative signal is therapeutically relevant for disorders associated with bone loss.

Keywords: BMP/mineralization/osteocyte/osteoporosis/*SOST*

Introduction

Anti-resorptives dominate the available treatments for disorders of bone loss, such as osteoporosis, but have modest effects on anabolic bone formation. With the approval of parathyroid hormone (Forteo™), the first anabolic agent to increase bone density has entered the market. However, there continues to be a need for alternative therapies to increase bone mass safely.

Human genetic diseases of the skeleton provide a route to identify genes that modulate the anabolic phase, which could ultimately provide the basis for a new therapeutic strategy to treat individuals affected by bone loss disorders. For example, the identification of the high bone mass gene, LRP5, revealed the role of the Wnt pathway in bone formation (Gong *et al*., 2001; Little *et al*., 2002). Loss of function or deletions in or near the *SOST* gene, including sclerosteosis and Van Buchem's disease (Balemans *et al*., 2001; Brunkow *et al*., 2001), lead to bone disorders having symptoms directly attributed to dysregulation of the anabolic phase of bone remodeling. Of the two diseases, sclerosteosis (MIM 269500) presents as a severe and systemic skeletal disorder characterized by generalized progressive bone overgrowth (Truswell, 1958; Hansen, 1967; Beighton *et al*., 1976; Beighton, 1988), resulting in thicker than normal trabeculae and cortices, increased bone mineral density and increased bone strength (Stein *et al*., 1983; Hill *et al*., 1986). Polymorphisms in the region of the *SOST* gene were also reported to be associated with age-related changes in bone mineral density in post-menopausal women (A.Uitterlinden, unpublished observation) but not in perimenopausal women (Balemans *et al*., 2002). Combined, these clinical data suggest that *SOST* is an important regulator of bone homeostasis and that antagonizing this gene could provide a pathway to generate high quality bone.

The protein product of the *SOST* gene, sclerostin, was predicted to be a secreted glycoprotein with homology to the DAN family of bone morphogenetic protein (BMP) antagonists and more distantly to the BMP antagonist noggin (Brunkow *et al*., 2001). Expression and transfection studies with noggin, gremlin and dan have suggested roles for these proteins in bone homeostasis, specifically in the differentiation of, and bone formation by, osteoblastic cells (Gazzerro *et al*., 1998; Abe *et al*., 2000; Hanaoka *et al*., 2000; Pereira *et al*., 2000; Gaddy-Kurten *et al*., 2002). In a broader context, BMPs and BMP antagonists have described skeletal roles specifically in chondrocyte differentiation, joint formation and osteogenesis (Merino *et al*., 1999; Tsumaki *et al*., 2002; Zhang *et al*., 2002). Here we establish the molecular mechanism of sclerostin's action and the role of this regulatory protein in the anabolic axis through *in vitro* and *in vivo* studies.

Results

Binding of sclerostin to BMP family members

We postulated that sclerostin binds to BMPs and that this binding could be crucial for the control of bone formation. The absence of sclerostin in sclerosteosis patients could lead to excess bone deposition by providing unopposed BMP activity. We examined the ability of sclerostin to bind to BMP-5 and BMP-6 using immunoprecipitation methodology. Purified recombinant BMPs and other test proteins were incubated with FLAG-agarose beads in the absence or presence of FLAG-tagged human sclerostin. Unbound proteins were removed by washing and the

immunoprecipitates analyzed by gel electrophoresis and western blot analysis. BMP-5 and BMP-6 bound to sclerostin but not to the FLAG resin (Figure 1A). No specific binding was found with the transforming growth factor-β (TGF-β) family members, TGF-β1, 2 and 3 or glial cell-derived neurotrophic factor (GDNF; data not shown).

The kinetic parameters of the BMP–sclerostin interaction were characterized using surface plasmon resonance (Biacore). Human sclerostin was coupled to a CM5 sensor chip. Purified recombinant BMP-2, BMP-4, BMP-5, BMP-6 and BMP-7 were injected at various concentrations. The resulting binding curves were used to determine the on and off rates. Under the conditions used in the study, BMPs-2, -4, -5, -6 and -7 exhibited similar binding kinetics and affinities (K_D = 0.9–3.4 nM) (see table 1 of the Supplementary data available at *The EMBO Journal* Online). Rat sclerostin also bound BMP proteins with similar kinetics (data not shown). In comparison, the apparent K_D of human noggin-Fc for BMP-4 was reported to be 19 pM and that of follistatin for activin, 200 pM (Zimmerman *et al*., 1996). Competition studies between the BMP proteins indicate that these proteins compete for the same site on sclerostin (see Supplementary figure 1).

Sclerostin binding to BMP-6 is competitive with BMP binding to type I and type II BMP receptors or with the BMP antagonist, DAN

We next sought to determine if sclerostin binding to BMPs could prevent the binding of BMPs to their receptors and thus inhibit BMP activity. We established an enzyme-linked immunosorbent assay (ELISA)-based competition assay to characterize the sclerostin–BMP interaction. BMP-6 selectively interacted with the human sclerostin-coated surface with high affinity (Figure 1B, K_D = 3.4 nM). Rat sclerostin also bound to BMP-6 in this ELISA with a comparable K_D (data not shown). When BMP-6 was held at 11 nM in the presence of increasing amounts of BMP receptor IA (FC fusion construct), the type I BMP receptor–FC clearly competed with sclerostin for binding to BMP-6 (Figure 1C, IC_{50} = 114 nM). A 10-fold molar excess of the receptor to BMP was sufficient to reduce binding by ~50%. This competition was also seen with a BMP receptor II–FC fusion protein (Figure 1D, IC_{50} = 36 nM) and DAN (Figure 1E, IC_{50} = 43 nM). rActivin R1B–FC fusion protein, a TGF-β receptor family member that does not bind BMP, did not compete with sclerostin binding to BMP-6 (data not shown), supporting the specificity of our assay. Similar results were obtained using Biacore technology (data not shown). These data demonstrate that sclerostin binds specifically to BMP proteins and that this binding is competitive with the interaction of BMPs with type I and type II BMP receptors. We predict that the DAN/sclerostin family of BMP antagonists may inhibit the binding of BMPs to the BMP receptors by binding to BMP proteins and blocking overlapping type I and type II receptor-binding sites (Kirsch *et al*., 2000; Hart *et al*., 2002). In support of this model, both type I and type II receptor-binding sites on BMP-7 are blocked by the binding of the noggin BMP antagonist (Groppe *et al*., 2002).

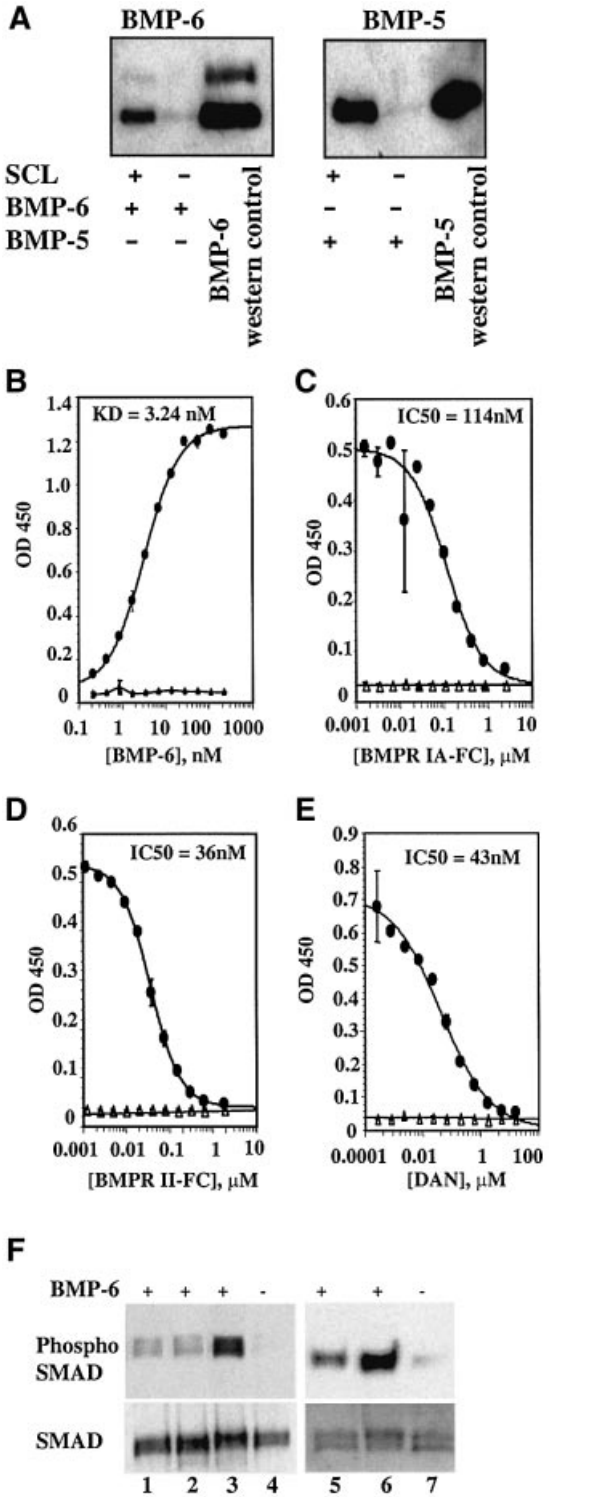

Fig. 1. Sclerostin is a BMP antagonist. (**A**) Co-immunoprecipitation of BMP-5 and BMP-6 with human sclerostin (SCL). (**B**) BMP-6 binding to human sclerostin (circles) or a BSA-blocked plate (triangles) in an ELISA-based association assay. (**C**) BMPRIA–FC competed with human sclerostin for BMP-6 binding. (**D**) BMPR II–FC competed with human sclerostin for BMP-6 binding. (**E**) The DAN BMP antagonist competed with human sclerostin for BMP-6 binding. (**F**) Inhibition of BMP-6-induced SMAD phosphorylation by human sclerostin. SMAD levels were constant in these lysates (anti-SMAD 1 and 5). Lane 1, treatment with anti-BMP-6 antibody; lane 2, BMPR1A–FC, lanes 3 and 4, no competitor added; lane 5, sclerostin; and lanes 6 and 7, no competitor added.

Sclerostin antagonism of BMP-stimulated SMAD phosphorylation

We next sought to determine if sclerostin would block early signal transduction by BMPs. BMP–BMP receptor complex formation induces the phosphorylation of SMADs 1, 5 or 8 (Fujii *et al*., 1999). The phosphorylation of SMADs in mouse mesenchymal C3H10T1/2 cells in response to BMP-6 can be seen by western blot using a phosphospecific anti-SMAD antibody (Figure 1F). This effect was blocked when incubations were performed in the presence of a goat polyclonal anti-BMP-6 antibody or BMP receptor 1A–FC (BMPR1A). When human sclerostin was pre-incubated with BMP-6 prior to addition to the cells, the BMP-6-induced SMAD phosphorylation was partially blocked. The ability of sclerostin to compete with the BMP receptors for BMP binding along with the data demonstrating sclerostin's ability to block early BMP-6-induced signaling (Figure 1C, D and F) together suggest a model whereby sclerostin inhibits BMP signal transduction by preventing BMP binding to its receptors.

SOST is expressed by osteogenic cells

We then determined which cell types expressed *SOST*. RNA was isolated from cultures of primary human osteoblasts, human mesenchymal cells (hMSCs) differentiated in culture to osteoblasts, and hypertrophic chondrocytes in cartilage tissue. These samples expressed the relevant phenotypic markers (i.e. type I collagen, *COL1A1*, for osteoblasts and type X collagen, *COLXA1*, for hypertrophic chondrocytes) and *SOST* (Figure 2A). On the other hand, undifferentiated hMSCs and adipocytes in adipose tissue expressed negligible levels of *SOST* (Figure 2A). Similar data were obtained using RNA isolated from hypertrophic chondrocytes and adipocytes generated in *in vitro* cultures of hMSCs (Pittenger *et al*., 1999) (data not shown). No expression of *SOST* was observed in RNA prepared from human osteoclasts or human osteoclast progenitor cells (see Supplementary figure 2) which contrasts with the findings reported elsewhere (Kusu *et al*., 2003). These results show that *SOST* is expressed by cells that are involved in osteogenesis and not in bone resorption.

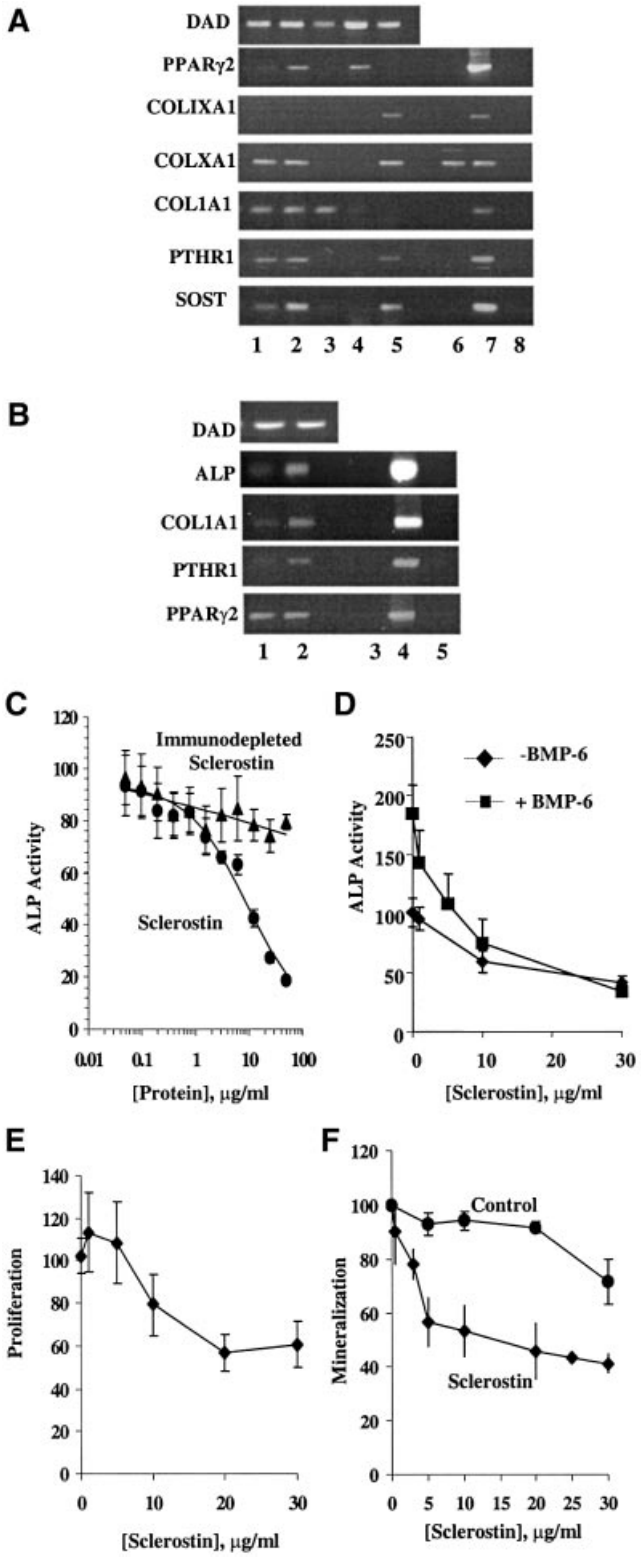

Fig. 2. *SOST* is expressed by osteoblasts. Sclerostin, the *SOST* gene product, decreased osteoblastic activity. (**A**) Expression of *SOST* in osteoblasts. RT–PCR analyses of RNA isolated from cultures of primary human osteoblasts (lane 1), hMSCs differentiated in culture to osteoblasts (lane 2), undifferentiated hMSCs (lane 3), abdominal adipose tissue (lane 4) and cartilage tissue (lane 5). PCR controls are shown in lanes 6 (genomic DNA), 7 (cDNA) and 8 (no DNA added). *DAD* served as a control for RNA loading. (**B**) Human sclerostin decreased the expression of osteoblastic phenotypic markers (*ALP*, *COL1A1* and *PTHR1*) in hMSCs grown in osteogenic medium. Lane 1, sclerostin-treated; 1ane 2, control protein preparation from Sf9 cells; PCR controls are shown in lanes 3 (genomic DNA), 4 (cDNA) and 5 (no DNA added). Sclerostin had no effect on non-osteoblastic markers such as *PPARγ2*. (**C**) Human sclerostin antagonized BMP-6-induced ALP activity in C3H10T1/2 cells. Sclerostin immunodepleted with an anti-FLAG antibody had no significant effects on BMP-6 stimulated ALP activity. Activity was expressed as mean ± SD, % activity in vehicle-treated cells (vehicle = 0.984 ± 0.201 OD_{405}/mg protein/30 min). (**D**) Human sclerostin antagonized the basal and BMP-6-induced ALP activities in hMSCs in a dose-dependent manner (ANOVA, $P < 0.0001$). Data shown represent mean ± SD, % activity in vehicle-treated cells (vehicle = 2.07 ± 0.21 OD/mg protein/5 min). (**E**) Human sclerostin significantly decreased the proliferation of hMSCs cultured in osteogenic medium as determined by [^{3}H]thymidine uptake (ANOVA, $P < 0.01$). Proliferation expressed as mean ± SD, % vehicle-treated cells (vehicle = 5806 ± 1300 c.p.m. per well). (**F**) Human sclerostin, but not the control Sf9 protein preparation, inhibited the mineralization of hMSCs grown in osteogenic medium in a dose-dependent manner (Kruskal–Wallis, $P < 0.0005$). Data shown represent the mean ± SD of mineralization (% vehicle, vehicle = 186.93 ± 75.96 μg calcium/mg protein).

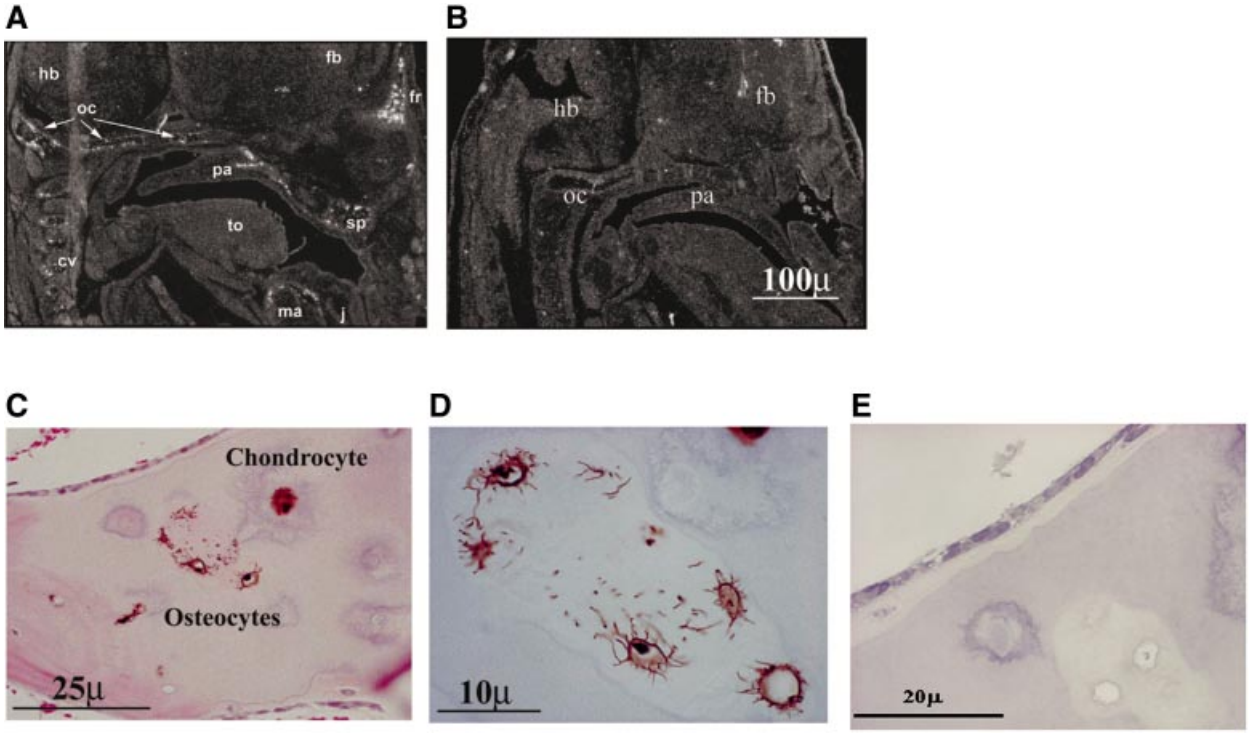

Fig. 3. Localization of the expression of *SOST* and sclerostin in murine and human bone tissues. (**A**) *In situ* analysis of *SOST* expression in 15.5-day-old mouse embryo. Hybridization with antisense RNA probes to *SOST* in the mouse embryo showed specific expression in the occipital (oc), frontal (fr) and sphenoid (sp) ossifying cartilages as well as the mandible (ma), palatal shelf of the maxilla (pa) and the cervical vertebrae (cv). (hb = hindbrain; fb = forebrain; j = jaw) (**B**) No signal was observed with the sense probe. (**C**) Immunohistochemical staining of normal adult human bone with a rabbit anti-human sclerostin antibody showed positive staining in osteocytes, osteocytic canaliculi and/or cell processes, and hypertrophic chondrocytes. H&E counterstain. (**D**) High power magnification of osteocytes and their cell processes/canaliculi in human bone that stain positive for sclerostin. (**E**) No staining for sclerostin was found using a rabbit IgG control antibody.

Sclerostin modulates osteoblastic function in mouse mesenchymal C3H10T1/2 and human osteoblasts

Mesenchymal and pre-osteoblastic cells grown in osteogenic medium differentiate into osteoblasts that express alkaline phosphatase (ALP) and form a mineralized extracellular matrix. The expression of osteoblastic phenotypic markers is altered by factors including BMPs (Wang *et al*., 1993; Oreffo *et al*., 1999; Suzawa *et al*., 1999; Deckers *et al*., 2002; van der Horst *et al*., 2002). We evaluated the effects of human sclerostin on the RNA levels of various osteoblastic markers in cultures of hMSCs differentiated into osteoblasts. RNA levels for parathyroid hormone receptor (*PTHR1*), *COL1A1* and *ALP* were significantly reduced, whereas levels of non-osteoblastic markers (e.g. the adipocyte marker, peroxisome proliferator-activated receptor, *PPARγ2*) were not affected in hMSCs treated with sclerostin (Figure 2B). We also evaluated the effect of sclerostin on the activities of several osteoblastic phenotypic markers. In C3H10T1/2 cells, BMP-6 induced ALP activity in a dose-dependent manner (data not shown). Sclerostin (human and rat proteins) effectively decreased BMP-6- and BMP-4-induced ALP activity in a dose-dependent manner ($P < 0.0001$) (Figure 2C, and data not shown). To verify the specificity of the sclerostin effect, the sclerostin-FLAG preparation was immunodepleted with an anti-FLAG antibody prior to addition to the cells. This treatment completely abolished the sclerostin-mediated antagonism of BMP-6 in the C3H10T1/2 cells (Figure 2C).

The BMP antagonism by sclerostin was confirmed further in a human cell model. In hMSCs, BMP-6 increased ALP activity ~2-fold (Figure 2D, value with BMP-6 only). Treatment of the cells with human sclerostin diminished the effect of BMP-6 on ALP activity in a dose-dependent manner ($P < 0.0001$, Figure 2D). Increasing concentrations of sclerostin also decreased ALP activity to below basal levels ($P < 0.005$, Figure 2D). These findings suggest that sclerostin antagonizes the effects of exogenously added BMPs and endogenously produced BMPs (hMSCs express BMPs- 2, -4 and -6; data not shown) as well as perhaps other cellular growth factors.

We next evaluated the effect of sclerostin on the proliferation and mineralization of cultures of hMSCs plated in osteogenic medium to initiate osteoblast differentiation. Human sclerostin significantly reduced the proliferation of, and the mineral deposition by, differentiating hMSCs in a dose-dependent manner ($P < 0.005$, Figure 2E and F, $P < 0.0005$). In parallel measurements, sclerostin also decreased the production of type I collagen protein (see Supplementary figure 3). Similar results were obtained using primary cultures of human osteoblasts (data not shown). These findings in conjunction with the observed effects on ALP activity suggest that sclerostin modulates the activity of osteoblasts.

SOST and sclerostin are expressed in osteocytes in mouse and human bones

In situ hybridization was used to localize the expression of *SOST* to specific cells in developing mice. *SOST* expres-

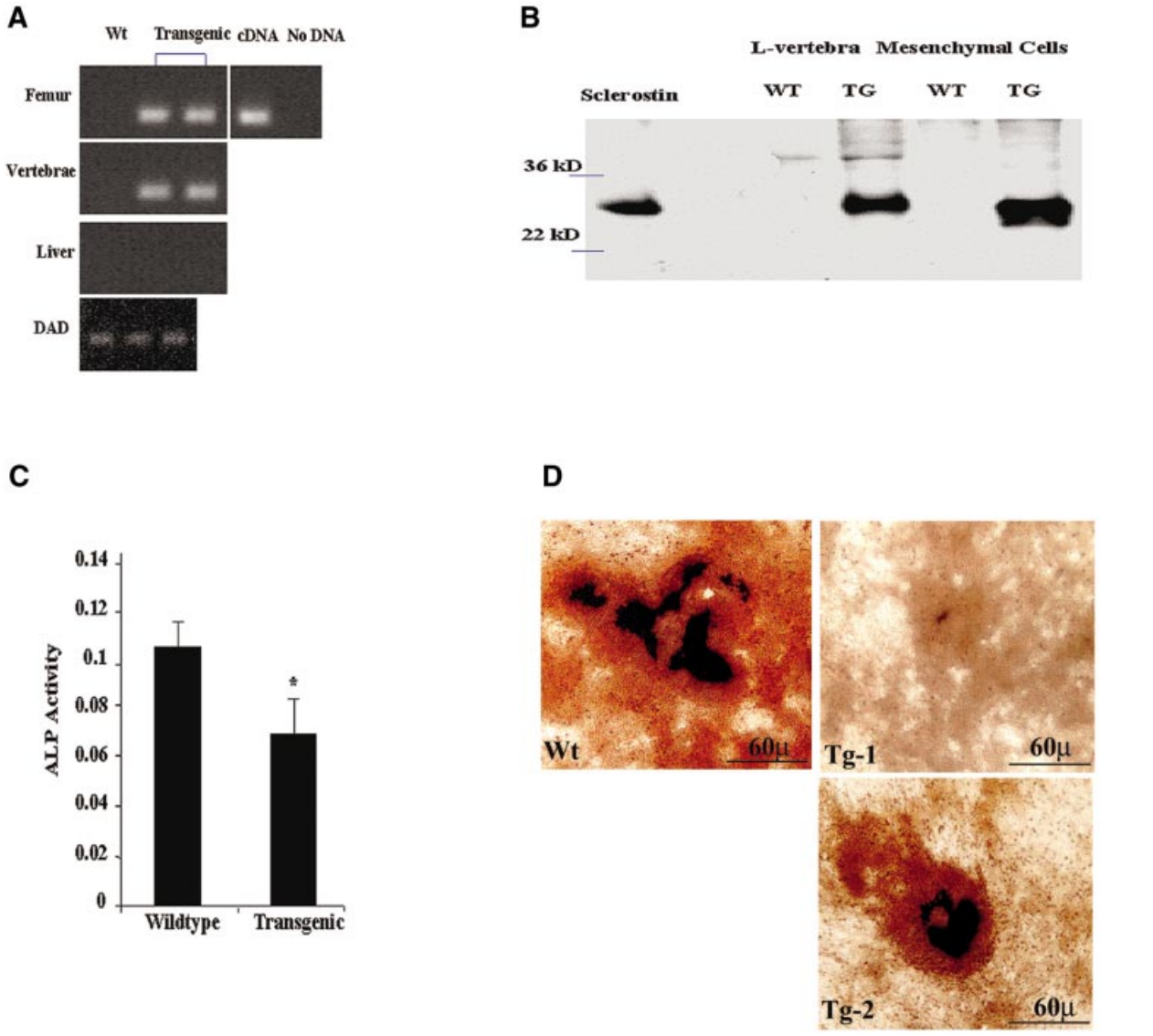

Fig. 4. Sclerostin-transgenic mice express *SOST* and sclerostin. (**A**) RT–PCR analyses of RNA isolated from femurs, lumbar vertebrae and liver of wild-type (Wt) littermates and transgenic mice. Bones from transgenic mice expressed the *SOST* transgene. *DAD* served as loading control. (**B**) Western blot analyses of protein extracts prepared from lumbar vertebrae and mesenchymal cells of wild-type (WT) and transgenic (TG) mice. Human sclerostin protein was expressed in bones and mesenchymal cells from TG mice. (**C**) Mesenchymal cells from transgenic mice cultured in osteogenic medium expressed lower levels of ALP activity (OD_{405}/mg protein/30 min) compared with cells from wild-type littermates ($P < 0.01$). (**D**) Varying levels of mineralization were observed in long-term cultures of mesenchymal cells from transgenic mice (Tg-1 and Tg-2) compared with cells from wild-type (Wt) mice. Cultures were stained with Von Kossa and alizarin red.

sion was observed in mineralizing tissues, for example the palate, mandible, rib, cervical vertebrae and the frontal, occipital and sphenoid ossifying cartilages of 15.5-day-old embryonic mice (Figure 3A and B). Immunohistochemical staining with rabbit monoclonal antibodies raised against human sclerostin was conducted on human bone. Osteocytes and osteocytic canaliculi and/or cell processes in both cortical and trabecular bone from normal adults showed strong positive staining for sclerostin (representative sample shown in Figure 3C–E). Staining was also observed in chondrocytes and weakly in other osteoblastic cells (Figure 3C). These findings agree with the results of our RT–PCR analyses (Figure 2A), demonstrating that the expression of *SOST* is associated with cells capable of osteogenesis.

Sclerostin-transgenic mice are osteopenic

We evaluated the function of sclerostin in an *in vivo* model by overexpressing human sclerostin in mice. Sclerostin-transgenic mice were generated by selectively targeting the expression of human *SOST* to bone with the mouse osteocalcin promoter, OG2 (Desbois *et al*., 1994). Four founders with copy numbers ranging from four to 30 were identified, two of which transmitted the transgene to their progeny. RT–PCR analyses of RNA and western blot analyses of protein samples and mesenchymal cells prepared from the bones of these animals showed that these mice expressed the transgene (Figure 4A) and human sclerostin protein (Figure 4B). We proceeded to characterize the phenotype of the mice. Mesenchymal cells were isolated from bones of transgenic and wild-type mice

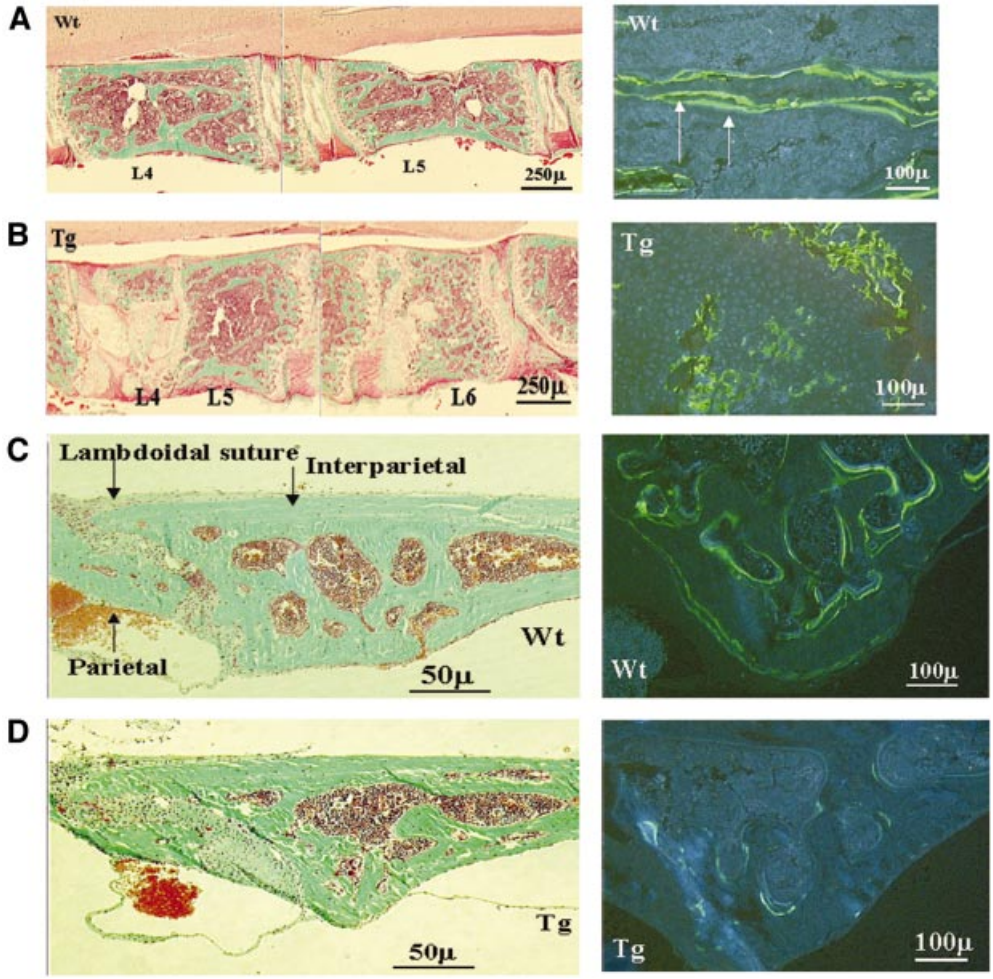

Fig. 5. Sclerostin-transgenic mice are osteopenic. (**A**) Left panel: lumbar vertebrae (L4 and L5) from a wild-type (Wt) littermate showing normal vertebral architecture. Goldner's trichrome stain for mineral deposition. Right panel: L4 from a wild-type littermate showing normal calcein double labeling (arrows). (**B**) Left panel: chondrodysplasia in L4–L6 of lumbar vertebrae from 6-week-old transgenic (Tg) mice. Vertebrae were also shorter, wider and lacked the normal trabecular and intervertebral disc architecture. Goldner stain. Right panel: fluorescence microscopy showing decreased calcein double labeling in L4 from transgenic mouse. Note the presence of hypertrophic chondrocytes, some calcified cartilage and lack of lamellar bone formation. (**C**) Left panel: calvarial section from a wild-type mouse showing parietal and interparietal bones. Goldner stain. Right panel: interparietal section showing normal calcein labeling. (**D**) Left panel: calvarial section from a transgenic mouse showing decreased bone volume. Goldner stain. Right panel: interparietal section showing markedly decreased calcein labeling.

and grown in osteogenic medium. ALP activity in mesenchymal cells from transgenic mice was significantly reduced compared with cells isolated from wild-type littermates ($P < 0.01$, Figure 4C). Long-term cultures of mesenchymal cells from transgenic mice exhibited varying levels of mineralization, but the levels were reduced compared with cultures from wild-type littermates (Figure 4D).

Analyses of histological sections of lumbar vertebrae showed that the overexpression of the human transgene was associated with disorganized architecture of the bone, thin cortices, reduced amounts of trabecular bone, impaired lamellar bone formation and chondrodysplasia (Figure 5A and B). Histomorphometrical analyses of calcein-labeled sections of L3 and L5 lumbar vertebrae showed significant differences between the transgenic and wild-type mice in the cartilage area (0.30 ± 0.06 mm^2 for transgenic versus 0.22 ± 0.06 mm^2 for wild-type, $P < 0.05$), the bone area (0.48 ± 0.05 cm^2 for transgenic versus 0.58 ± 0.09 cm^2 for wild-type, $P < 0.05$), and in the mineral apposition rate (2.07 ± 0.22 µm/day for transgenic versus 2.53 ± 0.19 µm/day for wild-type, $P < 0.01$). The calvariae from the transgenic mice also showed markedly decreased osteoid area (Goldner staining, left panels, Figure 5C and D) and decreased calcein labeling compared with wild-type mice (right panels, Figure 5C and D). Bone density scans of the vertebrae and femurs from both groups of mice showed that the bones of the transgenic mice contained less bone compared with their wild-type littermates (Figure 6A). The vertebrae and femurs of the transgenic mice were significantly more fragile and less resistant to fracture compared with bones of normal littermates ($P < 0.001$, Figure 6B and data not shown) after biomechanical testing by compression and four-point bending. In addition, histomorphometrical analyses of calcein-labeled calvarial bone sections showed that the bones of the transgenic mice had a significantly decreased osteoblast surface and a decreased bone formation rate compared with bones from wild-type mice (Figure 6C and D). There were no significant changes in

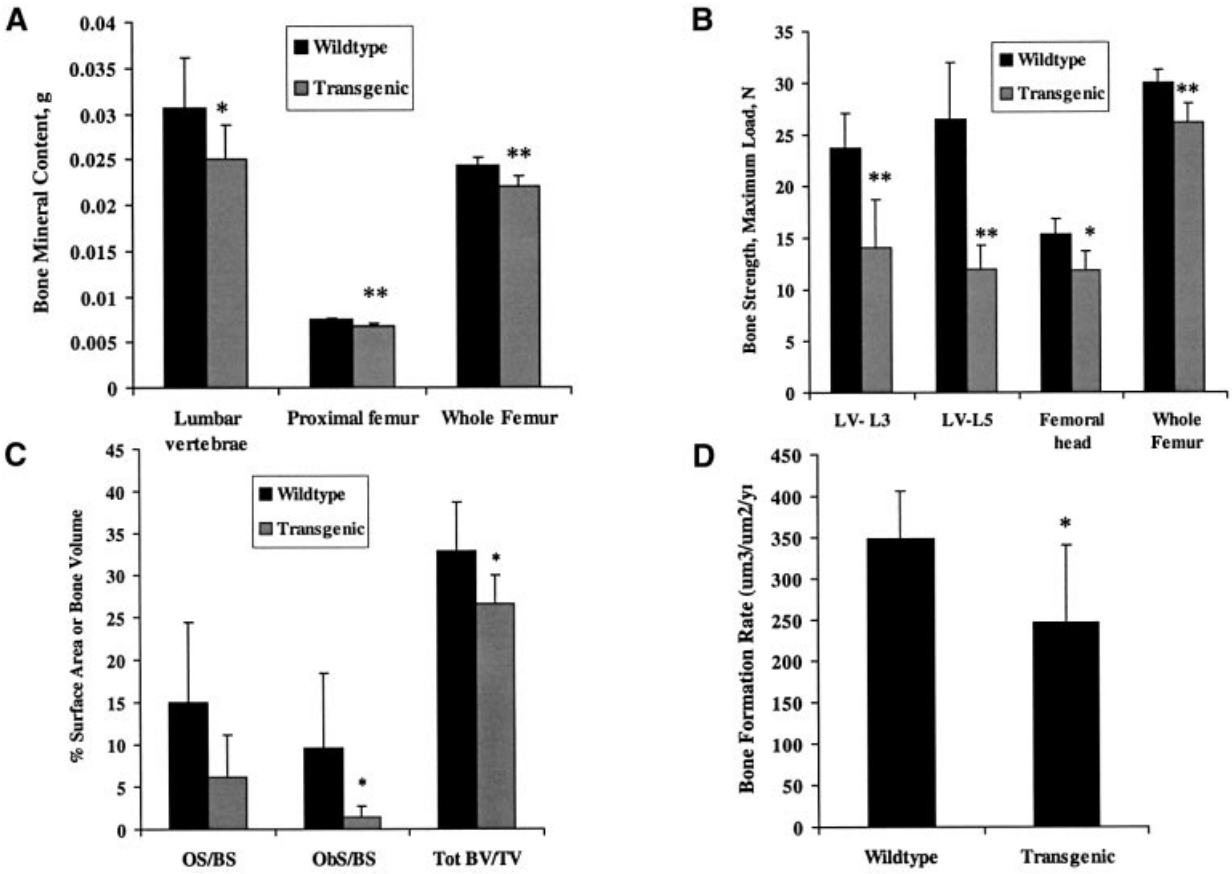

Fig. 6. Bones from sclerostin-transgenic mice contained less bone and were more fragile. (**A**) Bone mineral content of lumbar vertebrae and proximal femur/whole femur determined by PIXIMus was significantly lower in transgenic mice ($P < 0.05$ and $P < 0.01$, respectively) compared with those from wild-type littermates. (**B**) Lumbar vertebrae and femurs from sclerostin-transgenic mice were significantly more fragile than those from wild-type littermates ($P < 0.01$ and $P < 0.05$, respectively). Biomechanical analyses showed that less force (N) was needed to break the bones of transgenic mice. (**C**) Calvariae from sclerostin-transgenic mice exhibited less bone (osteoid) volume compared with bones from wild-type littermates ($P < 0.05$). Values were determined from analyses of Goldner-stained bone sections. OS = osteoid surface; BS = bone surface; ObS = osteoblast surface; BV = bone volume; TV = total volume. (**D**) Calvariae from sclerostin-transgenic mice exhibited a lower rate of bone formation compared with those from wild-type littermates ($P < 0.05$). Rates were determined from analyses of calcein-labeled bones.

the bone resorption parameters in any of the bone areas examined (data not shown). These findings all indicate that the overexpression of the human transgene in mice resulted in marked decreases in osteoblast activity and, therefore, decreased bone formation. These are the first data bridging the role of sclerostin in rodents with man where the gene was originally characterized. These results highlight the important role that sclerostin plays in bone formation and in maintaining bone integrity.

Discussion

The clinical observations in sclerosteosis suggest that the *SOST* mutation is one that targets a regulator of bone matrix formation (Stein *et al*., 1983; Hill *et al*., 1986). The cloning of *SOST* presented a mechanistic handle on an anabolic bone pathway relevant to the development of therapeutics for the treatment of bone disorders such as osteoporosis. In the current work, we have demonstrated that sclerostin is a BMP antagonist that interacts with a number of different BMPs and disrupts the biology of these proteins. Defining sclerostin as a BMP antagonist and the essential role that BMPs play in osteoblast differentiation and activity (Wang *et al*., 1993; Oreffo *et al*., 1999; Suzawa *et al*., 1999; Abe *et al*., 2000; Deckers *et al*., 2002; van der Horst *et al*., 2002) offers us insight into how bone formation may be regulated. However, sclerostin is distinct from the large family of BMP antagonists and noggin by virtue of its highly specific expression in osteogenic cells, in particular the osteocyte, and its strong association with osteogenesis.

Our findings depict the first instance whereby a genetically discovered regulator of bone density has been ascribed to the osteocyte. Osteocytes have been described as sensors that respond to mechanical and environmental stimuli and modulate the process of bone remodeling by fine-tuning the activities of osteoclasts and osteoblasts (Nomura and Takano-Yamamoto, 2000; Turner *et al*., 2002). These cells are connected to the osteoblastic lineage and represent an important final stage for a limited segment of the mature osteoblast population. Our *in vitro* studies have established that osteoblast differentiation is sensitive to sclerostin exposure. The data collectively suggest that sclerostin may serve as an integral connection for the osteocytic-mediated regulation of bone remodeling. We propose that sclerostin released from osteocytes could control the proliferation and differentiation of osteoprogenitor/pre-osteoblastic cells as well as the activity of mature osteoblasts by down-regulating BMP activity.

Given the sclerosteosis phenotype in humans, we predicted that in the sclerostin-transgenic mice, the overexpression of sclerostin would yield reduced bone formation and more fragile bones. Our data supported this premise, demonstrating a similarity in the sclerostin biology between rodents and humans. We envisage that the loss of sclerostin and the subsequent failure to regulate BMP action properly may in turn lead to increased numbers of activated osteoblasts and dysregulated growth of bone. Indeed, in sclerosteosis patients, there was elevated osteoblast activity manifested as high bone mass, increased thickness of cortical and trabecular bone, and increased bone strength (Stein *et al*., 1983; Hill *et al*., 1986). Furthermore, in both homozygotic and heterozygotic individuals, there is a pronounced life-long increase in bone formation due to altered sclerostin expression (Beighton, 1988; unpublished observations). These observations in conjunction with those from the transgenic mouse model demonstrate the powerful effect of BMP antagonists on bone density and skeletal morphogenesis. The absence of sclerostin in sclerosteosis is not compensated for by noggin or any other BMP antagonist, pointing to the central role that sclerostin plays in bone homeostasis via its control of osteoblast function.

While this manuscript was under review, a paper describing sclerostin activity and expression in embryonic and newborn mouse tissues was published (Kusu *et al*., 2003). Our findings contrast with the data in that paper in a number of ways. First, using *in situ* hybridization, RT–PCR and immunohistochemistry, we showed that sclerostin was expressed by osteogenic cell types including osteocytes. We report no expression of *SOST* in osteoclasts. In contrast, Kusu *et al*. (2003) used *in situ* data to show that *SOST* and *MMP-9* had similar expression patterns, leading them to conclude that *SOST* was expressed by osteoclasts and not osteoblasts. In our study, the high resolution images from immunohistochemistry were definitive in identifying osteocytes as the major *SOST*-expressing cell. There were also differences in the specificity and affinity of the sclerostin protein, probably due to differences in the protein preparations. It is of note that Kusu *et al*. (2003) reported that sclerostin's BMP antagonist activity was specific for BMP-6 and -7 as compared with BMP-2 and -4. However, we find that sclerostin will serve as an antagonist for all of these BMP proteins.

Methods to increase bone in man have long been sought. The bone formation axis controlled by sclerostin may provide an important new strategy to accomplish this outcome. Sclerostin, through genetics and the associated biology described here, asserts itself as a prime therapeutic target to address bone disorders. The modification of its activity or expression offers an exciting possibility for the development of new anabolics for the treatment of disorders associated with bone loss.

Materials and methods

PCR primers for RT–PCR

PCR primers to detect the expression of the human genes coding for *SOST*, *PTHR1*, *COL1A1*, *PPARγ2*, *ALP*, *COLIXA1*, *COLXA1* and the housekeeping gene, defender against death (*DAD*), are listed below. Primer sets crossed intron–exon boundaries to eliminate amplification of genomic DNA or generation of larger size amplicons. All PCR products were verified by sequencing.

Human *SOST* (product size 186 nucleotides): sense, 5′-CCGGAGCTGGAGAACAACAAG-3′; antisense, 5′-GCACTGGCCGGAGCACACC-3′. Human *PTHR1* (375 nucleotides): sense, 5′-AGGCCAGCCAGCATAATGGAA-3′; antisense, 5′-CTCCCGTTCACGAGTCTCAT-3′. Human *DAD* (626 nucleotides): sense, 5′-GCAGTTATGTCGGCGTCGGTA-3′; antisense, 5′-GTGGCATGGAGTTCTTTAATTTGGA-3′. Human *COL1A1* (216 nucleotides): sense, 5′-CACCAATCACCTGCGTACAG-3′; antisense, 5′-TGGTTTCTTGGTCGGTGG-3′. Human *ALP* (424 nucleotides): sense, 5′-CGC AGG ATT GGA ACA TCA-3′; antisense, 5′-GGC ATT GGT GTT GTA CGT CTT-3′. Human *COLIXA1* (765 nucleotides): sense, 5′-GAA AGG TGA CAG GGG TGT AG-3′; antisense, 5′-TTT GTT AAA TGC TCG CTG AC-3′. Human *COLXA1* (424 nucleotides): sense, 5′-CCGGGACCATCAGCTGTAG-3′; antisense, 5′-CCGGAAAACCTCTATCACCTT-3′. Human *PPARγ2* (375 nucleotides): sense, 5′-CTTCCGGAGAACAATCAGAT-3′; antisense, 5′-TCGCAGGCTCTTTAGAAACT-3′.

Expression and purification of sclerostin

Human *SOST* sequence was subcloned into pMelBac (Invitrogen, Carlsbad, CA) for transfer into a baculoviral expression vector. Recombinant baculoviruses expressing C-terminal FLAG-tagged sclerostin were purified according to the manufacturer's instructions.

For protein purification, conditioned medium was collected from infected Sf9 insect cells after 72 h and loaded onto a Heparin Hitrap column (Amersham Biosciences, Piscataway, NJ). The column was washed extensively with 150 mM NaCl in 50 mM HEPES pH 7.6 and the protein eluted by a 12-column volume gradient into 1 M NaCl in 50 mM HEPES pH 7.6. Positive fractions were pooled, brought to 10% glycerol and 1.4 mM β-mercaptoethanol (βME), and stored at –80°C. For a negative control, conditioned medium from an identical volume of uninfected cells was collected and processed as described above.

Alternatively, the positive fractions from the Heparin Hitrap column were pooled, dialyzed overnight into phosphate-buffered saline (PBS; pH 7.3) with 10% glycerol, and loaded onto an SP Hitrap column (Amersham). The protein was eluted with a 10-column volume gradient into PBS with 10% glycerol and 1 M NaCl. For a negative control, conditioned medium from an identical volume of uninfected cells was collected and processed as described above.

Rat sclerostin was produced using the DES *Drosophila* expression system according to the manufacturer's instructions (Invitrogen) and purified as described above for human sclerostin.

Rabbit monoclonal antibodies against rat and human sclerostin were raised by standard methods (Babcook *et al*., 1996).

Immunoprecipitation

Anti-FLAG M2 agarose beads (Sigma, St Louis, MO) were washed with IP buffer (20 mM Tris pH 7.6, 150 mM NaCl, 1 mM EDTA, 1% Triton X-100, 1.4 mM βME, 10% glycerol) before incubation in the presence or absence of 4 μg of sclerostin-FLAG. Unbound sclerostin-FLAG was removed by washing with IP buffer. The beads and tubes were blocked to prevent non-specific binding by pre-incubation with 5% bovine serum albumin (BSA) in PBS and washed with IP buffer. BMP-5 and -6 were rehydrated according to the manufacturer's (R&D Systems, Minneapolis, MN) instructions, diluted into IP buffer, and centrifuged to remove aggregated protein. The BMP solutions (5 μg/ml) were added to the beads with and without sclerostin-FLAG (4 μg) and incubated for 2 h to overnight at 4°C. The washed samples were analyzed on a 10–20% gradient Tris-glycine SDS–polyacrylamide gel (Novex, San Diego, CA), transferred to nitrocellulose, and the western blots developed with anti-BMP-5 or -6 antisera (RDI, Flanders, NJ).

ELISA

Nunc polysorp 96-well plates were coated overnight at 4°C with or without sclerostin-FLAG in PBS (300 ng of protein per well). The plates were blocked with 5% BSA in PBS, incubated with BMPs, washed, and developed using appropriate primary and horseradish peroxidase (HRP)-labeled secondary antibody reagents. Data analysis was performed using the Life Science Workbench (LSW) Data Analysis Toolbox (MDL Information Systems, San Leandro, CA).

For competition ELISAs, sclerostin-FLAG, BMP-binding protein DAN (R&D Systems) or BMP receptor–FC fusion proteins (R&D Systems) were added to the wells to compete with the absorbed sclerostin for BMP binding prior to the addition of 11 nM BMP. Development and data analyses were as described above.

Effects of sclerostin in mouse mesenchymal C3H10T1/2 cells

C3H10T1/2 cells (American Type Culture Collection, Manassas, VA), plated in 96-well dishes (25 000 cells/well) in Dulbecco's modified Eagle's medium supplemented with high glucose and glutamine, 10% fetal calf serum (FCS), 1% penicillin/streptomycin, 0.1 mM non-esssential amino acids, 1 mM sodium pyruvate, 55 μM βME and 20 mM HEPES pH 7.3, were used to determine the effects of sclerostin on BMP-induced ALP activity. Human sclerostin-FLAG or rat sclerostin (0–50 μg/ml) was pre-incubated with 500 ng/ml BMP-6 in medium for 1 h prior to addition to cells. Cells were harvested 72 h later for assay of ALP activity (Pierce, Rockford, IL) by determining the amount of *p*-nitrophenol synthesized from *p*-nitrophenylphosphate ($OD_{405\ nm}$/mg protein/30 min of incubation at room temperature). To test the specificity of the sclerostin effect, sclerostin-FLAG was pre-incubated for 2 h at 4°C with anti-FLAG M2 agarose beads. The mixture was spun at 10 000 *g* for 15 min at 4°C and the supernatant treated as 'sclerostin' in the above assay.

To assay for SMAD phosphorylation, confluent 6-well plates of C3H10T1/2 cells were serum depleted overnight in medium containing 1% FCS. BMP-6 was pre-incubated in medium with or without BMP antagonists (40 μg/ml BMP R1A–FC, 15 μg/ml human sclerostin-FLAG) or antibodies (40 μg/ml) for 1 h at room temperature prior to addition to cells. After 30 min, the plates were washed with ice-cold PBS and the cells harvested with SDS–PAGE loading buffer. Western blot analysis was performed with anti-phospho-SMAD 1, 5 and 8 (Cell Signaling Technologies, Beverly, MA) and anti-SMAD 1 and 5 (Santa Cruz Biotechnology, Santa Cruz, CA) antibodies.

Effects of sclerostin in hMSC cells

To determine the effect of sclerostin on ALP activity, hMSCs (Cambrex Bioscience, Walkersville, MD) cultured in osteogenic medium (MSCGM with 100 nM dexamethasone, 50 μg/ml ascorbic acid and 10 mM β-glycerophosphate βGP) were treated with BMP-6 (500 ng/ml) and increasing concentrations of sclerostin-FLAG. BMP-6 with sclerostin-FLAG were pre-incubated in media at room temperature for 30 min prior to addition to cells. Cultures were harvested after 6 days for assay of ALP activity. For proliferation studies, cells treated with sclerostin protein were pulsed with 2.5 μCi/ml [methyl-^{3}H]thymidine (25 Ci/mmol, Amersham Bioscience) for 24 h. To determine the effect of sclerostin on mineralization, sclerostin-FLAG (0 to 30 μg/ml) was added to cultures of hMSCs 8 days after plating. Two weeks later, mineralization was assessed by measuring calcium deposition (Sigma calcium assay).

In other experiments, hMSCs were plated in osteogenic medium to assess the effect of sclerostin on RNA levels of osteoblastic phenotypic markers. The cells, treated with sclerostin-FLAG (10 μg/ml) or control (protein purified from conditioned medium of Sf9 cells), were harvested 40 h later and RNA prepared (Stratagene, Hayward, CA) for RT–PCR analyses of *PTHR1*, *COL1A1*, *ALP* and *PPARγ2*.

SOST expression in human and mouse mesenchymal cells

hMSCs cultured in growth (undifferentiated hMSCs) or osteogenic (hMSCs to osteoblasts) medium were harvested 21 days after plating and RNA isolated for RT–PCR analyses of *SOST*, *COL1A1*, *PPARγ2*, *PTHR1*, *COLIXA1* and *COLXA1*. *SOST* expression was also determined in RNA prepared from abdominal adipose tissue (Biochain Institute, Hayward, CA), cartilage tissue from femoral growth plates (Biochain Institute), primary cultures of human osteoblasts (Cambrex Bioscience), adipocytes and chondrocytes from 28 day cultures of hMSCs (Pittenger *et al*., 1999), and in human osteoclast precursor cells and human osteoclasts (Cambrex Bioscience).

Radioactive in situ hybridization

Mouse embryos (15.5 days old) were fixed in 4% phosphate-buffered formaldehyde pH 7.2 overnight, dehydrated and embedded in paraffin. Sections (5 μm thick) were prepared and *in situ* hybridization performed by Phylogeny, Inc. (Columbus, OH) using [^{35}S]UTP-(>1000 Ci/mmol, Amersham Bioscience) labeled sense and antisense *SOST* RNA probes (Lyons *et al*., 1990).

Immunohistochemistry

Paraffin blocks of human bone tissue samples were acquired from the Peterborough Hospital Human Research Tissue Bank (Peterborough, UK). The tissues were obtained after surgical treatment and fixed in 4% neutral-buffered formalin prior to decalcification in EDTA solution. Paraffin sections (7 μm thick) of decalcified bone were deparaffinized with xylene and graded ethanols prior to treatment with 6% H_2O_2 and proteinase K. The primary rabbit anti-human sclerostin 23E03 antibody (259 μg/ml) was diluted 1:50 in 5% non-fat dry milk in PBS–Tween-20 and incubated with tissue sections for 2 h at room temperature. Control slides were treated with rabbit IgG (R&D Systems). Detection was performed using goat anti-rabbit HRP-linked IgG (DAKO, Carpinteria, CA) and the peroxidase substrate/chromogen solution Vector® NovaRed™ (Vector Laboratories, Inc., Burlingame, CA) as directed by the manufacturers. The sections were counterstained with hematoxylin QS (Vector Laboratories), dehydrated in an ethanol series, cleared in xylene and mounted with Permount (Fisher Scientific, Pittsburgh, PA).

Sclerostin-transgenic mice

Animal studies were conducted following PHS guidelines. The transgene construct was assembled in the pBlueScript KS+ cloning vector (Stratagene) and included the following elements: the 1000 bp *Bam*HI fragment including the mouse osteocalcin gene 2 (*OG2*) promoter/enhancer (GenBank accession No. U66848; Desbois *et al*., 1994), obtained from genomic DNA using PCR primers 5′-GGATCCGC-GCCGCTTCATTTCATTTCCACCTAGAG-3′ and 5′-GGATCCTCCA-GTAGCATTTATATCGGC-3′; the 1185 bp *Bam*HI–*Eco*RI fragment from the human *APO E* gene including the first coding exon, the first intron and part of the second exon (GenBank accession No. AF261279), obtained from genomic DNA using PCR primers 5′-GGATCCA-GGAGTCCAGATCC-3′ and 5′-GAATTCCCTGCCTGTGATTGG-3′; and a 661 bp *Hin*dIII–*Xho*I fragment corresponding to the coding sequence of the human *SOST* gene, obtained by RT–PCR using primers 5′-AAGCTTGGTACCATGCAGCTCCCAC-3′ and 5′-CTCGAGCTA-GTCGGCGTTCTCCAG-3′ (GenBank accession No. AF326739). Transgenic mice were generated by oocyte microinjection (Xenogen Biosciences, Cranbury, NJ) using a *Not*I fragment isolated from the construct described above. Transgene transmission was determined by PCR and Southern blot analysis. To determine the RNA and protein levels of the transgene, bones and liver were removed from transgenic mice (copy number = 10). The tissues were quick-frozen in liquid nitrogen, ground into powder using a pestle and mortar, and extracted with Trizol reagent (Invitrogen) according to the manufacturer's directions. Mesenchymal cells were isolated from the femurs and tibiae of transgenic and wild-type mice using a Ficoll gradient (Sigma) and cultured as previously described (Abe *et al*., 2000; Gaddy-Kurten *et al*., 2002). ALP activity, mineral deposition, and RNA and protein extracts were prepared from the mesenchymal cells as described above. Human *SOST* levels in the tissue and cell samples were determined by RT–PCR. Human sclerostin protein was detected by western blot analysis using a specific anti-human sclerostin antibody.

Female transgenic (copy number = 10) and wild-type littermates (6 weeks of age) were injected with 15 mg/kg calcein 7 and 2 days before sacrifice. Animals were euthanized under anesthesia. Lumbar and sacral vertebrae and calvariae were collected and processed for methyl methacrylate embedding. The tissue blocks were processed and sectioned sagitally for histomorphometry (SkeleTech, Inc., Bothell, WA). Additionally, lumbar vertebrae and femurs were harvested from 10- to 12-week-old mice for biomechanical studies (Akhter *et al*., 2001; SkeleTech, Inc.).

Supplementary data

Supplementary data are available at *The EMBO Journal* Online.

Acknowledgements

The authors are grateful to Angie Snell and Lyudmila Karpik for their help with the sclerostin-transgenic mice, and to the SLAM group and the Protein Expression Group at Celltech Seattle for their help with the anti-human sclerostin antibodies. We also thank Rutger van Bezooijen and Clemens Löwik for sharing data prior to publication.

References

Abe,E., Yamamoto,M., Taguchi,Y., Lecka-Czernik,B., O'Brien,C.A., Economides,A.N., Stahl,N., Jilka,R.L. and Manolagas,S.C. (2000) Essential requirement of BMPs-2/4 for both osteoblast and osteoclast formation in murine bone marrow cultures from adult mice: antagonism by noggin. *J. Bone Miner. Res.*, **15**, 663–673.

Akhter,M.P., Cullen,D.M., Gong,G. and Recker,R.R. (2001) Bone biomechanical properties in prostaglandin EP1 and EP2 knockout mice. *Bone*, **29**, 121–125.

Babcook,J.S., Leslie,K.B., Olsen,O.A., Salmon,R.A. and Schrader,J.W.

(1996) A novel strategy for generating monoclonal antibodies from single, isolated lymphocytes producing antibodies of defined specificities. *Proc. Natl Acad. Sci. USA*, **93**, 7843–7848.

Balemans,W. *et al*. (2001) Increased bone density in sclerosteosis is due to the deficiency of a novel secreted protein (SOST). *Hum. Mol. Genet.*, **10**, 537–543.

Balemans,W., Foernzler,D., Parsons,C., Ebeling,M., Thompson,A., Reid,D.M., Lindpaintner,K., Ralston,S.H. and Van Hul,W. (2002) Lack of association between the SOST gene and bone mineral density in perimenopausal women: analysis of five polymorphisms. *Bone*, **31**, 515–519.

Beighton,P. (1988) Sclerosteosis. *J. Med. Genet.*, **25**, 200–203.

Beighton,P., Durr,L. and Hamersma,H. (1976) The clinical features of sclerosteosis. A review of the manifestations in twenty-five affected individuals. *Ann. Intern. Med.*, **84**, 393–397.

Brunkow,M.E. *et al*. (2001) Bone dysplasia sclerosteosis results from loss of the SOST gene product, a novel cystine knot-containing protein. *Am. J. Hum. Genet.*, **68**, 577–589.

Deckers,M.M., van Bezooijen,R.L., van der Horst,G., Hoogendam,J., van Der Bent,C., Papapoulos,S.E. and Lowik,C.W. (2002) Bone morphogenetic proteins stimulate angiogenesis through osteoblast-derived vascular endothelial growth factor A. *Endocrinology*, **143**, 1545–1553.

Desbois,C., Hogue,D.A. and Karsenty,G. (1994) The mouse osteocalcin gene cluster contains three genes with two separate spatial and temporal patterns of expression. *J. Biol. Chem.*, **269**, 1183–1190.

Fujii,M. *et al*. (1999) Roles of bone morphogenetic protein type I receptors and Smad proteins in osteoblast and chondroblast differentiation. *Mol. Biol. Cell*, **10**, 3801–3813.

Gaddy-Kurten,D., Coker,J.K., Abe,E., Jilka,R.L. and Manolagas,S.C. (2002) Inhibin suppresses and activin stimulates osteoblastogenesis and osteoclastogenesis in murine bone marrow cultures. *Endocrinology*, **143**, 74–83.

Gazzerro,E., Gangji,V. and Canalis,E. (1998) Bone morphogenetic proteins induce the expression of noggin, which limits their activity in cultured rat osteoblasts. *J. Clin. Invest.*, **102**, 2106–2114.

Gong,Y. *et al*. (2001) LDL receptor-related protein 5 (LRP5) affects bone accrual and eye development. *Cell*, **107**, 513–523.

Groppe,J. *et al*. (2002) Structural basis of BMP signalling inhibition by the cystine knot protein Noggin. *Nature*, **420**, 636–642.

Hanaoka,E., Ozaki,T., Nakamura,Y., Moriya,H., Nakagawara,A. and Sakiyama,S. (2000) Overexpression of DAN causes a growth suppression in p53-deficient SAOS-2 cells. *Biochem. Biophys. Res. Commun.*, **278**, 20–26.

Hansen,H. (1967) Sklerosteose. In Opitz,H. and Schmid,F. (eds), *Handbuch der Kinderheilkunde*. Springer-Verlag, Berlin, Vol. **6**, pp. 351–355.

Hart,P.J., Deep,S., Taylor,A.B., Shu,Z., Hinck,C.S. and Hinck,A.P. (2002) Crystal structure of the human TβR2 ectodomain–TGF-β3 complex. *Nature Struct. Biol.*, **9**, 203–208.

Hill,S.C., Stein,S.A., Dwyer,A., Altman,J., Dorwart,R. and Doppman,J. (1986) Cranial CT findings in sclerosteosis. *Am. J. Neuroradiol.*, **7**, 505–511.

Kirsch,T., Sebald,W. and Dreyer,M.K. (2000) Crystal structure of the BMP-2–BRIA ectodomain complex. *Nature Struct. Biol.*, **7**, 492–496.

Kusu,N., Laurikkala,J., Imanishi,M., Usui,H., Konishi,M., Miyake,A., Thesleff,I. and Itoh,N. (2003) Sclerostin is a novel secreted osteoclast-derived bone morphogenetic protein antagonist with unique ligand specificity. *J. Biol. Chem.*, **278**, 24113–24117.

Little,R.D. *et al*. (2002) A mutation in the LDL receptor-related protein 5 gene results in the autosomal dominant high-bone-mass trait. *Am. J. Hum. Genet.*, **70**, 11–19.

Lyons,G.E., Schiaffino,S., Sassoon,D., Barton,P. and Buckingham,M. (1990) Developmental regulation of myosin gene expression in mouse cardiac muscle. *J. Cell Biol.*, **111**, 2427–36.

Merino,R., Rodriguez-Leon,J., Macias,D., Ganan,Y., Economides,A.N. and Hurle,J.M. (1999) The BMP antagonist Gremlin regulates outgrowth, chondrogenesis and programmed cell death in the developing limb. *Development*, **126**, 5515–5522.

Nomura,S. and Takano-Yamamoto,T. (2000) Molecular events caused by mechanical stress in bone. *Matrix Biol.*, **19**, 91–96.

Oreffo,R.O., Kusec,V., Romberg,S. and Triffitt,J.T. (1999) Human bone marrow osteoprogenitors express estrogen receptor-α and bone morphogenetic proteins 2 and 4 mRNA during osteoblastic differentiation. *J. Cell. Biochem.*, **75**, 382–392.

Pereira,R.C., Economides,A.N. and Canalis,E. (2000) Bone morphogenetic proteins induce gremlin, a protein that limits their activity in osteoblasts. *Endocrinology*, **141**, 4558–4463.

Pittenger,M.F. *et al*. (1999) Multilineage potential of adult human mesenchymal stem cells. *Science*, **284**, 143–147.

Stein,S. *et al*. (1983) Sclerosteosis: neurogenetic and pathophysiologic analysis of an American kinship. *Neurology*, **33**, 267–277.

Suzawa,M., Takeuchi,Y., Fukumoto,S., Kato,S., Ueno,N., Miyazono,K., Matsumoto,T. and Fujita,T. (1999) Extracellular matrix-associated bone morphogenetic proteins are essential for differentiation of murine osteoblastic cells *in vitro*. *Endocrinology*, **140**, 2125–2133.

Truswell,A.S. (1958) Osteopetrosis with syndactyly, a morphologic variant of Albers–Schonberg disease. *J. Bone Joint Surg. (Br.)*, **40**, 208–218.

Tsumaki,N., Nakase,T., Miyaji,T., Kakiuchi,M., Kimura,T., Ochi,T. and Yoshikawa,H. (2002) Bone morphogenetic protein signals are required for cartilage formation and differently regulate joint development during skeletogenesis. *J. Bone Miner. Res.*, **17**, 898–906.

Turner,C.H., Robling,A.G., Duncan,R.L. and Burr,D.B. (2002) Do bone cells behave like a neuronal network? *Calcif. Tissue Int.*, **70**, 435–442.

vanderHorst,G., van Bezooijen,R., Deckers,M., Hoogendam,J., Visser,A., Lowik,C. and Karperien,M. (2002) Differentiation of murine pre-osteoblastic KS483 cells depends on autocrine BMP signalling during all phases of osteoblast formation. *Bone*, **31**, 661–669.

Wang,E.A., Israel,D.I., Kelly,S. and Luxenberg,D.P. (1993) Bone morphogenetic protein-2 causes commitment and differentiation in C3H10T1/2 and 3T3 cells. *Growth Factors*, **9**, 57–71.

Zhang,D., Ferguson,C.M., O'Keefe,R.J., Puzas,J.E., Rosier,R.N. and Reynolds,P.R. (2002) A role for the BMP antagonist chordin in endochondral ossification. *J. Bone Miner. Res.*, **17**, 293–300.

Zimmerman,L.B., De Jesus-Escobar,J.M. and Harland,R.M. (1996) The Spemann organizer signal noggin binds and inactivates bone morphogenetic protein 4. *Cell*, **86**, 599–606.

Received March 11, 2003; revised September 12, 2003; accepted October 10, 2003